UDC 621.771.8
https://doi.org/10.17073/0021-3438-2025-4-37-49

Research article
Научная статья

Finite element modeling and analysis of the technological feasibility of a new cladding scheme for aluminum-lithium alloy 1441 ingots

A.M. Pesin[1], **A.V. Razinkin**[2], **V.A. Zamaraev**[2], **D.O. Pustovoitov**[1]

[1] **Nosov Magnitogorsk State Technical University**
38 Lenin Ave., Magnitogorsk, Chelyabinsk Region 455000, Russia

[2] **PJSC "Kamensk-Uralsky Metallurgical Plant"**
5 Zavodskaya Str., Kamensk-Uralsky, Sverdlovsk Region 623405, Russia

✉ Denis O. Pustovoitov (pustovoitov_den@mail.ru)

Abstract: Using the QForm software package, a finite-element analysis was conducted to assess the technological feasibility of implementing a new cladding scheme for 360-mm-thick aluminum–lithium alloy 1441 ingots under the production conditions of PJSC "KUMP". Instead of the traditional cladding scheme, in which the cladding plates are roll-bonded to the ingot over four passes with an absolute reduction of 6 mm per pass, the cladding plates are seated in pre-machined recesses milled into the top and bottom surfaces of the ingot and roll-bonded in a single pass with an absolute reduction of 24 mm. The analysis showed that the new cladding scheme prevents extrusion of the cladding plates from the ingot surface at high reductions, enabling the use of thinner plates (10 mm instead of the conventional 15 mm). The new approach also significantly reduces the total number of passes and inter-deformation pauses during rough rolling, thereby improving the thermal condition of the workpiece before finish rolling. A reduction of three passes and three pauses (10 s each) leads to an average temperature increase of approximately 23 °C. The deformation behavior of the base metal (alloy 1441) and the cladding layer (ACpl alloy) was analyzed. The mean accumulated strain in the ingot after rolling according to the new scheme was found to be twice as high as under the traditional scheme, while the deformation distribution within the cladding layer was more uniform. The obtained results can be used to enhance and optimize hot-rolling parameters for clad sheets and strips of aluminum–lithium alloy 1441 at PJSC "KUMP".

Keywords: aluminum-lithium alloy 1441, hot rolling, cladding, deformation state, finite-element modeling, stress-strain state, temperature.

Acknowledgements: The research was supported by the Russian Science Foundation (Grant No. 23-79-30015) and co-funded under Agreement No. KK0987F-2023.

For citation: Pesin A.M., Razinkin A.V., Zamaraev V.A., Pustovoitov D.O. Finite element modeling and analysis of the technological feasibility of a new cladding scheme for aluminum-lithium alloy 1441 ingots. *Izvestiya. Non-Ferrous Metallurgy*. 2025;31(4):37–49.
https://doi.org/10.17073/0021-3438-2025-4-37-49

Конечно-элементное моделирование и анализ технологической возможности применения новой схемы плакирования слитков из алюминий-литиевого сплава 1441

А.М. Песин[1], **А.В. Разинкин**[2], **В.А. Замараев**[2], **Д.О. Пустовойтов**[1]

[1] **Магнитогорский государственный технический университет им. Г.И. Носова**
Россия, 455000, Челябинская обл., г. Магнитогорск, пр-т Ленина, 38

[2] **ПАО «Каменск-Уральский металлургический завод»**
Россия, 623405, Свердловская обл., г. Каменск-Уральский, ул. Заводская, 5

✉ Денис Олегович Пустовойтов (pustovoitov_den@mail.ru)

Аннотация: С использованием программы «QForm» проведен конечно-элементный анализ технологической возможности применения новой схемы плакирования слитков толщиной 360 мм из алюминий-литиевого сплава 1441 в условиях ПАО «КУМЗ». Взамен традиционной схемы плакирования, предусматривающей приварку планшетов к слитку за 4 прохода с абсолютными обжатиями по 6 мм, предложено укладывать планшеты в специальные углубления, предварительно выполненные фрезерованием на верхней и нижней поверхностях слитка, а приварку осуществлять за 1 проход с абсолютным обжатием 24 мм. Показано, что новая схема плакирования позволяет предотвратить выдавливание планшетов с поверхности слитка при высоких абсолютных обжатиях. Это дает возможность использовать более тонкие планшеты (толщиной 10 мм) взамен традиционных (15 мм). Установлено, что по новой схеме плакирования существенно сокращается общее количество проходов и междеформационных пауз при черновой прокатке и за счет этого улучшается тепловое состояние раската перед чистовой прокаткой. При сокращении 3 проходов и 3 междеформационных пауз среднее повышение температуры составляет ≈23 °C. Исследовано деформированное состояние основного металла (сплав 1441) и плакирующего слоя (сплав АЦпл). Показано, что средняя накопленная деформация в слитке (математическое ожидание) после прокатки по новой схеме в 2 раза выше в сравнении с традиционной схемой. При этом характер деформации плакирующего слоя при прокатке по новой схеме более равномерный. Результаты могут быть использованы для совершенствования и оптимизации технологических режимов горячей прокатки плакированных листов и полос из алюминий-литиевого сплава 1441 в условиях ПАО «КУМЗ».

Ключевые слова: алюминий-литиевый сплав 1441, горячая прокатка, плакирование, режимы деформации, моделирование методом конечных элементов, напряженно-деформированное состояние, температура.

Благодарности: Исследования выполнены за счет гранта Российского научного фонда (соглашение № 23-79-30015) и в рамках договора о софинансировании № КК0987F-2023.

Для цитирования: Песин А.М., Разинкин А.В., Замараев В.А., Пустовойтов Д.О. Конечно-элементное моделирование и анализ технологической возможности применения новой схемы плакирования слитков из алюминий-литиевого сплава 1441. *Известия вузов. Цветная металлургия.* 2025;31(4):37–49. https://doi.org/10.17073/0021-3438-2025-4-37-49

Introduction

Compared with conventional aluminum alloys such as D16 (AA2024 analogue), aluminum—lithium alloys possess a unique combination of properties, including lower density, higher stiffness, superior strength and fatigue resistance, as well as good corrosion resistance and satisfactory weldability [1—7]. The full technological cycle for manufacturing sheets and strips from aluminum—lithium alloys has been developed and industrially implemented at the Kamensk-Uralsky Metallurgical Plant Joint Stock Company (KUMZ JSC), which remains the only producer and supplier of these alloys in Russia. Aluminum—lithium alloy 1441 of the Al—Cu—Mg—Li system belongs to the second generation of Al—Li alloys; its production at KUMZ JSC began in 1990 [8]. This structural alloy is widely used in aircraft and spacecraft manufacturing [9—13].

Cladding is a distinct hot-rolling operation intended to cover ingots of aluminum alloys with a thin layer of pure aluminum (≥ 99.3 %) or the ACpl alloy to ensure additional corrosion protection [14, 15]. In the case of aluminum—lithium alloys, cladding also significantly increases the product yield by improving edge and surface quality of sheets and strips [16].

Three main cladding types are distinguished [17]:

— technological cladding (B), aimed at creating more favorable deformation conditions during rolling of low-ductility alloys (cladding-layer thickness not exceeding 1.5 % of sheet thickness);

— normal cladding (A), providing corrosion protection (cladding-layer thickness of at least 2 % for sheets thicker than 1.9 mm, and at least 4 % for thinner sheets);

— thickened cladding (U), ensuring enhanced corrosion protection (layer thickness of at least 4 % for sheets thicker than 1.9 mm, and 8 % or more for thinner sheets).

For the production of clad sheets and strips from aluminum—lithium alloy 1441, flat ingots with cross-sections of 225×950 mm, 275×1100 mm, 300×1100 mm, 390×1360 mm are used [8]. Before rolling, both the ingot (base-metal blank) and the cladding plates (blanks of cladding metal) undergo special preparation. To remove casting defects and ensure high-quality two-sided (top and bottom) roll-bonding of the plates, the wide faces of the ingots are milled by 5—15 mm per side [17]. The mating surfaces of the ingot and plates are then degreased. The plate thickness (h_{pl}) s calculated from the ingot thickness (H_{ing}) and the required cladding-layer thickness [17]:

$$h_{pl} = H_{ing}\delta/100a + 2\delta, \qquad (1)$$

where a = 0.8 is a coefficient accounting for the difference in deformation of the ingot and the plates in the first passes, and δ is the upper limit of cladding-layer thickness specified in the relevant standards.

Before hot rolling, the aluminum—lithium 1441 ingots with the attached cladding plates are heated to no more than 460 °C. Roll-bonding of the plates is carried out during the first four passes with an absolute reduction per pass not exceeding 6 mm in cylindrical rolls, without applying a lubricant—coolant mixture (LCM). The LCM is intentionally excluded during these first passes to prevent its penetration under the plates and the formation of sub-plate blisters. In subsequent roughing and finishing passes, rolling is performed with the application of a water—oil emulsion containing 1—2.5 % rolling oil.

According to [4], the recommended temperature range for hot rolling of aluminum—lithium alloy 1441 is 460—390 °C. However, under industrial conditions the actual range is 460—340 °C for rough rolling and 340—300 °C (or even lower) for finish rolling. The temperature drop results from heat losses during a large number of roughing passes (up to 19) and the corresponding inter-pass delays, when the workpiece cools in air. Intensifying deformation during rough rolling is limited by the roll-bonding stage, at which the absolute reduction per pass must not exceed 6 mm (≈ 1.5 % relative reduction); otherwise, extrusion of the plate material from the ingot surface occurs.

Numerous studies [18—27] have been devoted to improving the cladding process for aluminum alloys during hot rolling; nevertheless, the issue of increasing the efficiency of plate bonding to the ingot remains unresolved.

The aim of the present work is to perform finite-element modeling and analyze the technological feasibility of applying a new cladding scheme for aluminum—lithium 1441 ingots in order to reduce the number of passes and inter-pass pauses during rough rolling.

Materials and methods

Finite element modeling and analysis of the co-rolling process of the ingot (base-metal blank) with two cladding plates (blanks of cladding metal) placed on the top and bottom surfaces were carried out using the QForm 11.0.1 software package in a two-dimensional plane-strain formulation (license No. R0-U2497-170719U197, licensee — Nosov Magnitogorsk State Technical University). The ingot material was aluminum—lithium alloy 1441 (Al—1.7 Cu—0.8 Mg—1.8 Li). The initial state corresponded to the condition after single-stage homogenization annealing at 450 °C for 8 h.

Experimental data on the flow stress of alloy 1441 were obtained from hot torsion tests on a Gleeble 3800 thermomechanical simulator equipped with a Torsion module. Cylindrical specimens of total length 165 mm and diameter 14 mm were used, with a working zone length L = 20 mm and radius R = 5 mm. One specimen end was rigidly fixed, while a torque was applied to the other (rotating) end. Tests were conducted at 450, 400, 350, 300, and 250 °C with strain rates of 0.01, 1, 10, and 50 s^{-1}. The flow-stress curves of alloy 1441, described by the relationship

$$\sigma_s = f(\bar{\varepsilon}, \dot{\varepsilon}, t), \qquad (2)$$

where $\bar{\varepsilon}$ is the equivalent strain; $\dot{\varepsilon}$ is the strain rate (s^{-1}); t is the temperature (°C), were approximated by a tabulated function.

The cladding layer material was aluminum alloy ACpl (97.8 %), with a chemical composition in accordance with GOST 4784-2019. As an example, Fig. 1 presents the flow-stress curves of aluminum—lithium alloy 1441 and the ACpl alloy at a strain rate of 10 s^{-1} and various temperatures.

The simulation was performed under the operating conditions of the Quarto 4600 roughing mill stand of the hot-rolling facility at KUMZ JSC. According to the traditional process, roll-bonding of the cladding plates is carried out during the first four passes according to a cross-rolling scheme, where the length of the ingot becomes its width after edge-turning (rotation by 90°). Therefore, for the two-dimensional finite element model, the following initial dimensions of the ingot after milling were adopted: 360×1360 mm (thickness × length). The ingot had a rectangular shape without chamfers or corner rounding. The initial dimensions of the cladding plates were 15×1100 mm (thickness × length). The total dimensions of the ingot with the top and bottom plates placed on it were 390×1360 mm (thickness × length). Hot rolling was simulated in working rolls of 1150 mm diameter. The ingot with the plates was heated to 450 °C in a furnace. The transfer time from the heating furnace to the rolling stand was empirically taken as 8 min. The rolling speed in each roughing pass was assumed to be 1 m/s, and the inter-pass pause was 10 s.

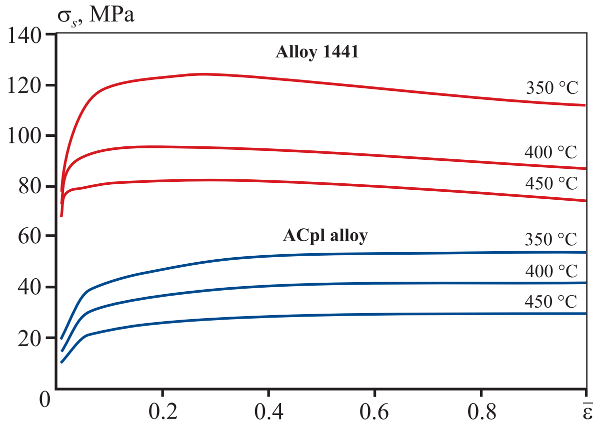

Fig. 1. Flow-stress curves of aluminum—lithium alloy 1441 and ACpl alloy at a strain rate of 10 s^{-1} and different temperatures

Рис. 1. Кривые сопротивления деформации алюминий-литиевого сплава 1441 и алюминиевого сплава АЦпл при скорости деформации 10 c^{-1} и различных температурах

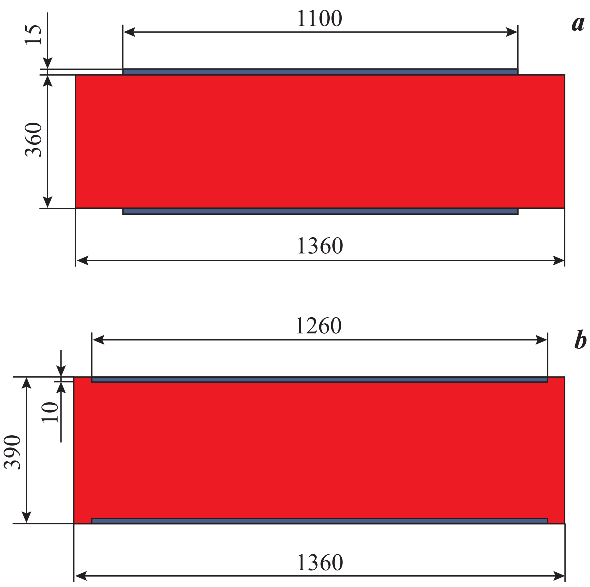

Fig. 2. Traditional (***a***) and new (***б***) schemes cladding plate placement schemes on the ingot

Рис. 2. Традиционная (***a***) и новая (***b***) схемы укладки планшетов на слиток

To describe frictional conditions at the contact with the rolls, Levanov's friction law was used:

$$\tau = mk(1 - e^{-1.25\sigma_n/\sigma_s}), \qquad (3)$$

where τ is the shear friction stress (MPa); m is the friction factor; σ_n is the normal contact pressure (MPa); σ_s is the flow stress (MPa); and k is the maximum shear stress (MPa), proportional to σ_s according to the relationship $k = \sigma_s/\sqrt{3}$.

Since roll-bonding of the plates is carried out without a lubricant—coolant mixture, the friction factor at the contact between the work rolls and the workpiece was taken as $m = 0.95$.

For the contact between the aluminum—lithium alloy 1441 ingot and the ACpl alloy plates during the bonding stage, the same Levanov friction law (Eq. 3) was applied with $m = 1$.

Finite-element modeling was used to compare two cladding schemes: 1) the traditional scheme (Fig. 2, *a*), in which cladding plates are placed on the flat top and bottom faces of the ingot and roll-bonded over four passes with an absolute reduction of 6 mm per pass; and 2) the new scheme (Fig. 2, *b*), in which the plates are seated in pre-machined recesses milled into the top and bottom faces and roll-bonded in a single pass with an absolute reduction of 24 mm.

Results and discussion

During the 8-minute transfer of the ingot with cladding plates from the heating furnace, where the temperature was 450 °C, to the rolling stand, the workpiece cooled in air. The calculated temperature field of the ingot with plates before rolling is shown in Fig. 3.

Because of the large difference in the geometric dimensions of the ingot and the plates, particular attention was paid to mesh refinement of the modeled objects. Fig. 4 shows the general view of the finite-element mesh. The maximum element sizes were as follows: global — no more than 30 mm; local — no more than 10 mm; and in the contact zone (Fig. 5) — no more than 1 mm. For the rolls along a 90° arc, the minimum number of elements was set to 180.

The temperature fields after roll-bonding the plates to the ingot for both cladding schemes are presented in Fig. 6. The mean ingot temperature (mathematical expectation) after four passes with absolute reductions of 6 mm was 399 °C (Fig. 7, *a*). After rolling in a single pass with an absolute reduction of 24 mm, the mean temperature was 422 °C (Fig. 7, *b*).

Thus, reducing three passes and, accordingly, three inter-pass pauses of 10 s each results in an average temperature increase of about 23 °C for the rough-rolled workpiece.

Although the absolute reduction per pass in the traditional scheme is quite small (only 6 mm), extrusion of the cladding plates from the ingot surface still occurs (Fig. 6, *a*). This effect arises because deformation is largely localized in the softer cladding layer (ACpl alloy) rather than penetrating into the stronger ingot core (alloy 1441).

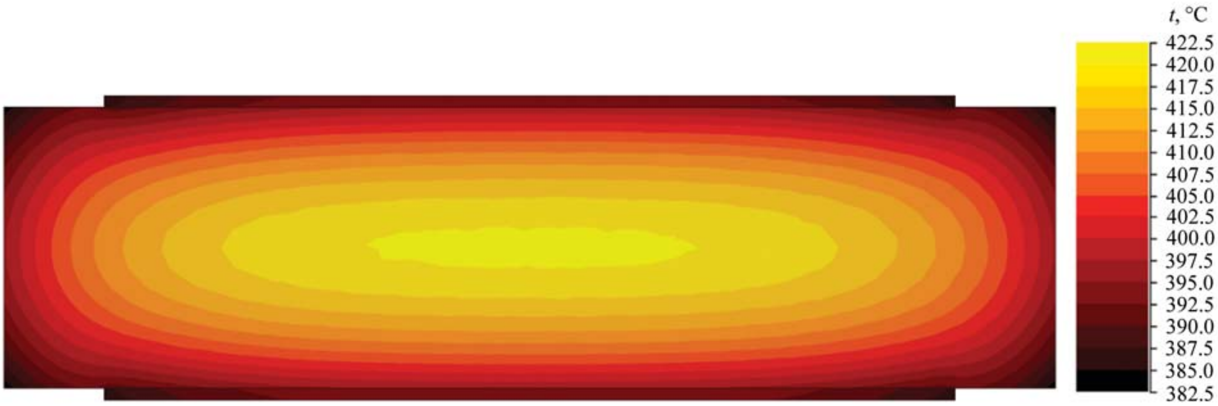

Fig. 3. Temperature field of the ingot with cladding plates before rolling

Рис. 3. Температурное поле слитка с планшетами перед началом прокатки

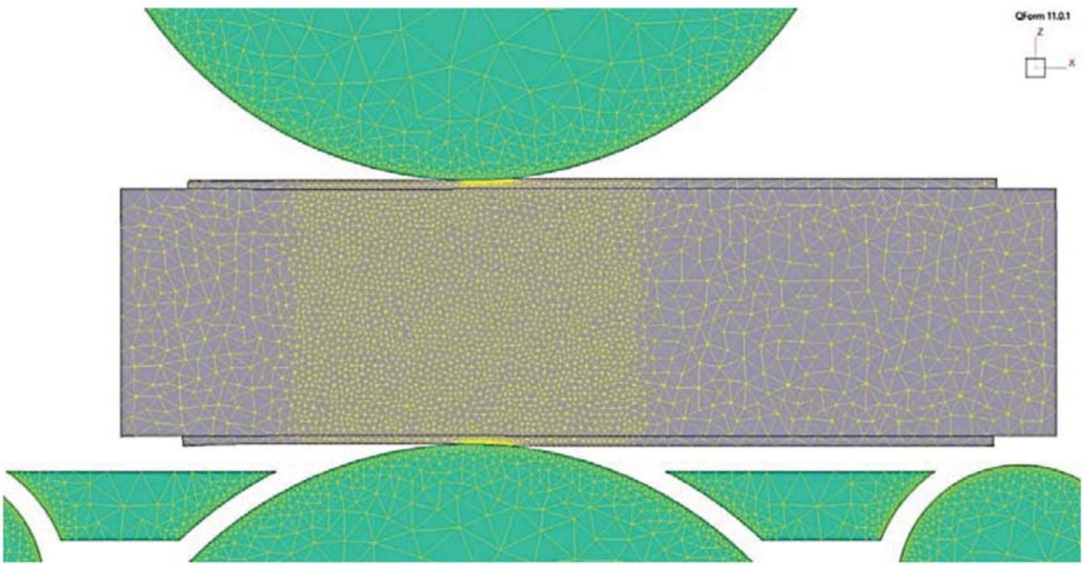

Fig. 4. General view of the finite-element mesh

Рис. 4. Общий вид сетки конечных элементов

The change in cladding-layer thickness during rolling differs significantly between the two schemes (Fig. 8). After four passes with reductions of 6 mm, the cladding-layer thickness decreases from the initial 15 mm to 8.8 mm. After rolling in a single pass with a 24 mm reduction, the thickness decreases from 10 mm to 9.3 mm. These results confirm that the new cladding scheme prevents plate extrusion from the ingot surface even under high absolute reductions, thereby allowing the use of thinner plates (10 mm instead of 15 mm).

The total initial thickness of the ingot with plates (390 mm) and the total absolute reduction (24 mm) were identical for both schemes. However, the deformation state of the base metal (alloy 1441) and the cladding layer (ACpl alloy) differed substantially (Fig. 9).

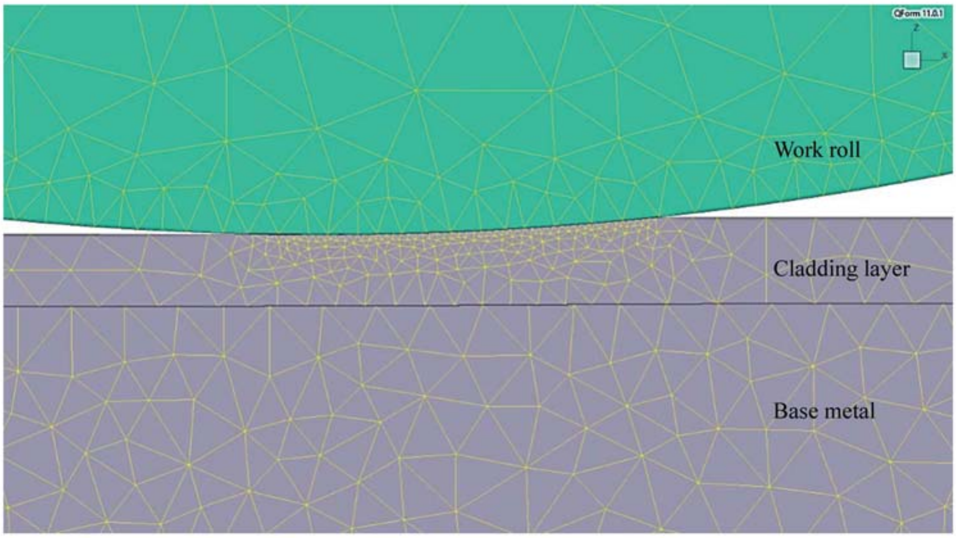

Fig. 5. Finite-element mesh in the contact zone

Рис. 5. Сетка конечных элементов в зоне контакта

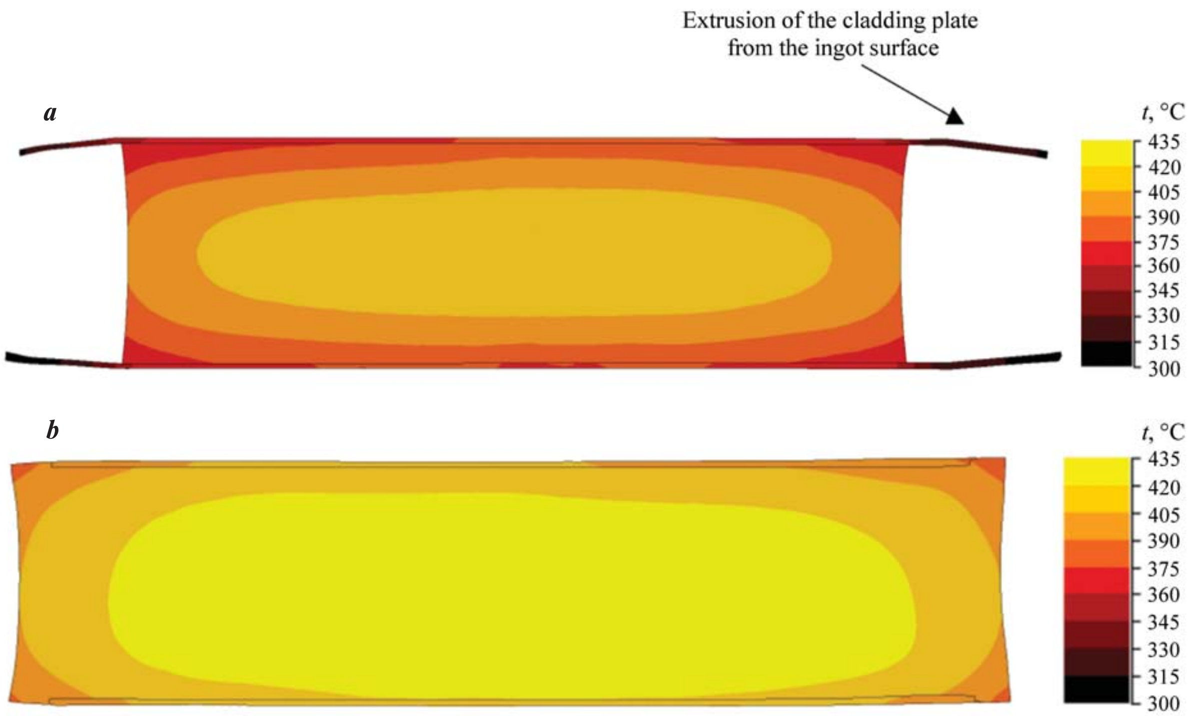

Fig. 6. emperature field after roll-bonding of cladding plates to the ingot for the traditional (***a***) and the new (***b***) schemes

Рис. 6. Температурное поле после приварки планшетов к слитку по традиционной (***a***) и новой (***b***) схемам

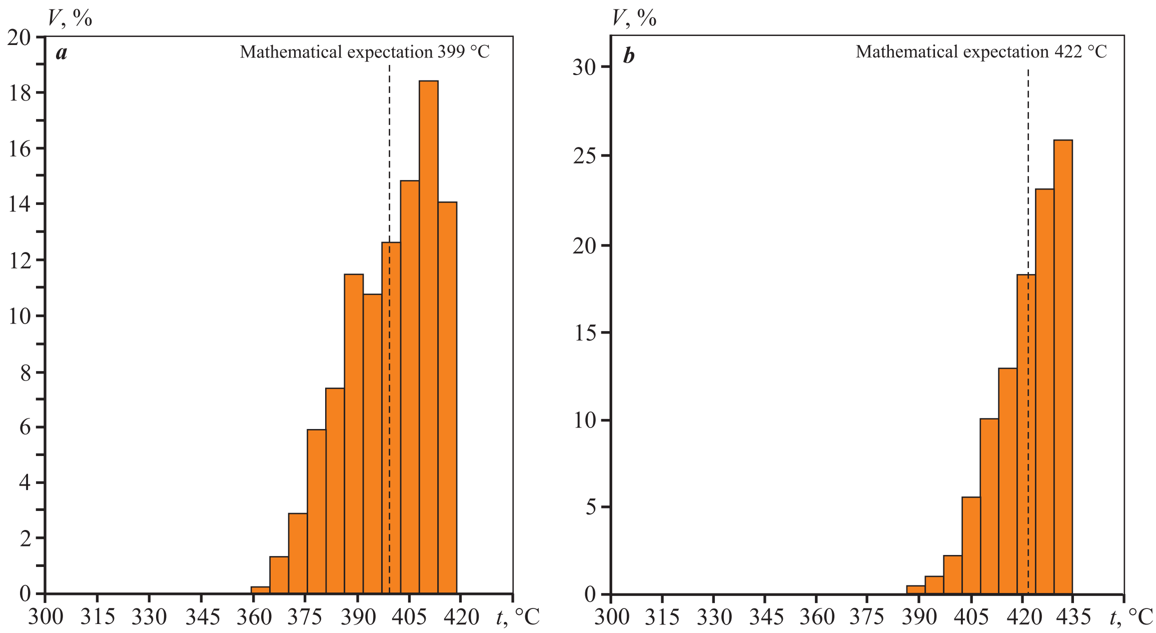

Fig. 7. Temperature distribution histograms over the ingot volume (V) after roll-bonding according to the traditional (***a***) and the new (***b***) schemes

Рис. 7. Гистограммы распределения температуры по объему (V) слитка после приварки планшетов по традиционной (***a***) и новой (***b***) схемам

The deformation state was characterized by the accumulated plastic strain ($\bar{\varepsilon}$), a dimensionless integral quantity. In QForm, the accumulated strain $\bar{\varepsilon}$ was calculated by numerical integration of the strain-rate intensity at each node [28]:

$$\bar{\varepsilon} = \sum_n \dot{\bar{\varepsilon}}^n \Delta b_n, \tag{4}$$

where $\dot{\bar{\varepsilon}}^n$ is the strain-rate intensity (s^{-1}); Δb_n is the time-step increment (s), and n is the number of calculation steps.

The mean accumulated strain in the ingot (mathematical expectation) after four passes with reductions of 6 mm was 0.05 (Fig. 10, *a*). After a single-pass rolling with a 24 mm reduction, it doubled to 0.10 (Fig. 10, *b*).

In the cladding layer, on the contrary, the mean accumulated strain (mathematical expectation) after rolling according to the traditional scheme was higher — 0.98 (Fig. 11, *a*) — compared with 0.66 after rolling according to the new scheme (Fig. 11, *b*). Comparing the strain-distribution histograms in Fig. 11 shows that deformation in the cladding layer is more uniform when rolling is performed according to the new scheme.

For the Quarto 4600 roughing stand of KUMZ JSC, the energy—force parameters of both schemes were evaluated. Because 2D modeling does not account for spread, the total strip width was assumed constant at 3300 mm. According to the simulation, in the traditional four-pass scheme (6 mm per pass), the maximum rolling forces ranged from approximately 21200 kN in the first pass to 25100 kN in the fourth (Fig. 12). For the new single-pass scheme with a 24 mm reduction, the maximum force was about 34000 kN (Fig. 12).

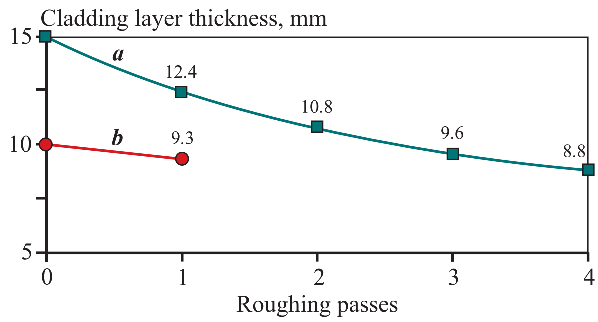

Fig. 8. Variation in cladding-layer thickness after rolling according to the traditional (***a***) and the new (***b***) schemes

Рис. 8. Изменение толщины плакирующего слоя по проходам после прокатки по традиционной (***a***) и новой (***b***) схемам

Importantly, the calculated rolling forces for both schemes did not exceed the permissible limit of

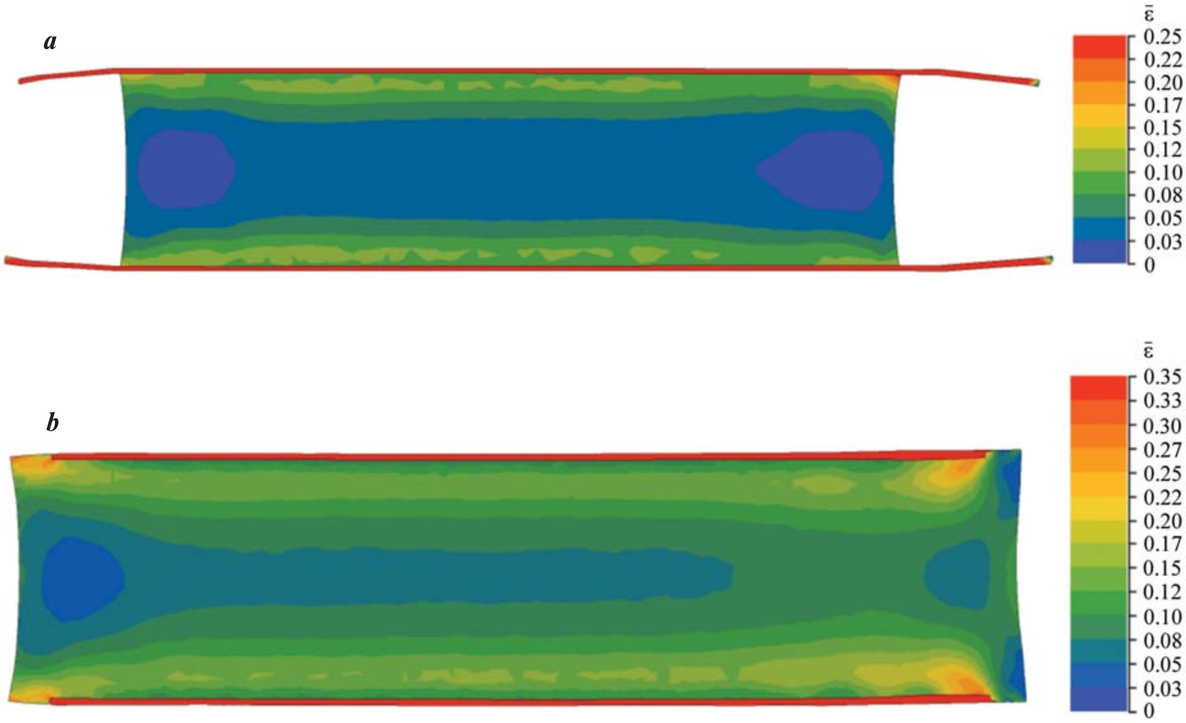

Fig. 9. Strain field after rolling according to the traditional (***a***) and the new (***b***) schemes

Рис. 9. Поле деформаций после прокатки по традиционной (***a***) и новой (***b***) схемам

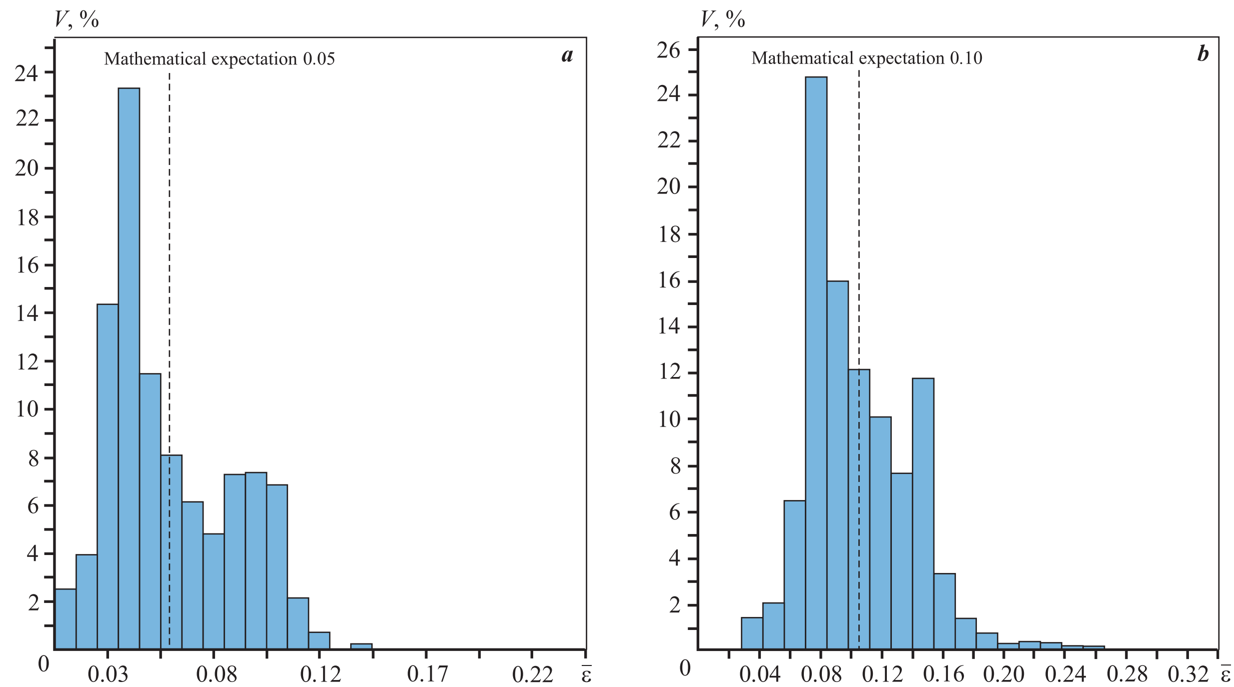

Fig. 10. Distribution histograms of accumulated strain ($\bar{\varepsilon}$) over the ingot volume (V) (base metal) after rolling according to the traditional (***a***) and the new (***b***) schemes

Рис. 10. Гистограммы распределения накопленной деформации ($\bar{\varepsilon}$) по объему (V) слитка (основного металла) после прокатки по традиционной (***a***) и новой (***b***) схемам

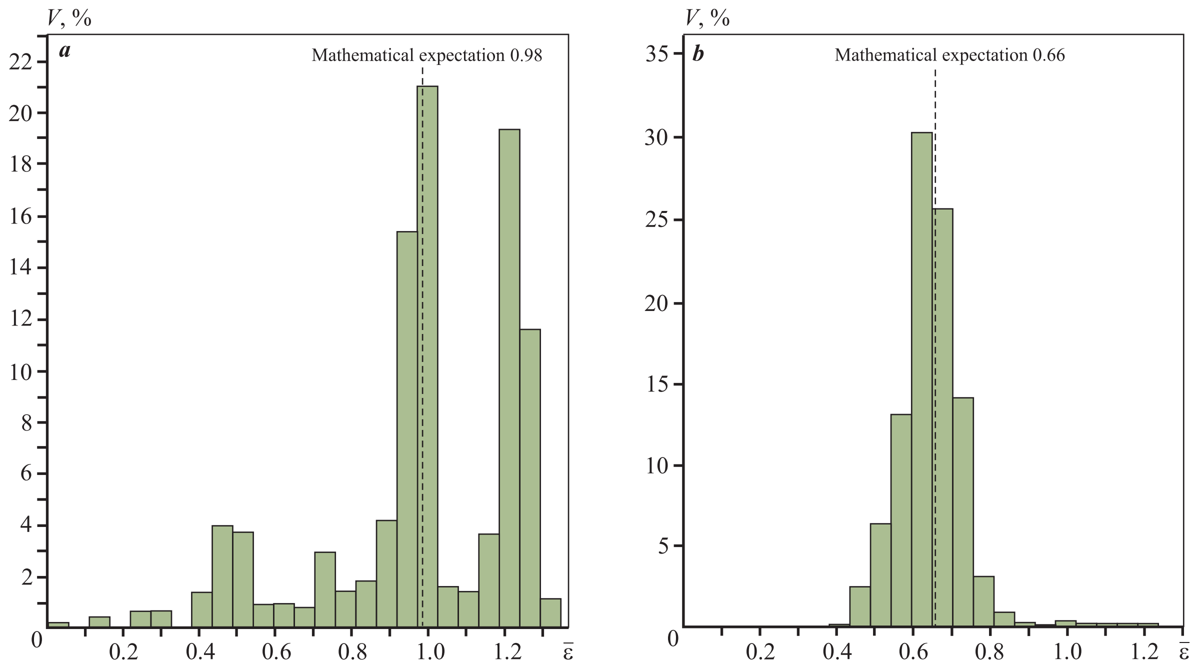

Fig. 11. Distribution histograms of accumulated strain over the cladding-layer volume (V) after rolling according to the traditional (***a***) and the new (***b***) schemes

Рис. 11. Гистограммы распределения накопленной деформации ($\bar{\varepsilon}$) по объему (V) плакирующего слоя после прокатки по традиционной (***а***) и новой (***b***) схемам

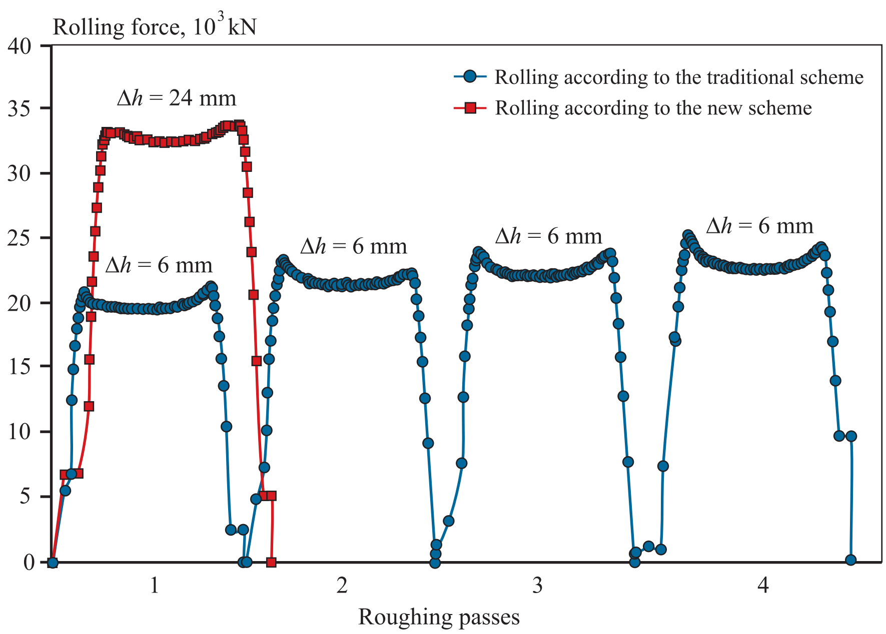

Fig. 12. Rolling forces in the traditional and new cladding schemes

Рис. 12. Усилия при прокатке по традиционной и новой схемам

80 000 kN, corresponding to the rated capacity of the Quarto 4600 roughing stand at KUMZ JSC.

Therefore, the finite-element analysis confirms the technological feasibility of the proposed cladding scheme for aluminum—lithium alloy 1441 ingots. For flat ingots of 390 × 1360 mm, implementation of the new scheme requires adjustment of the milling configuration on the wide faces (Fig. 13).

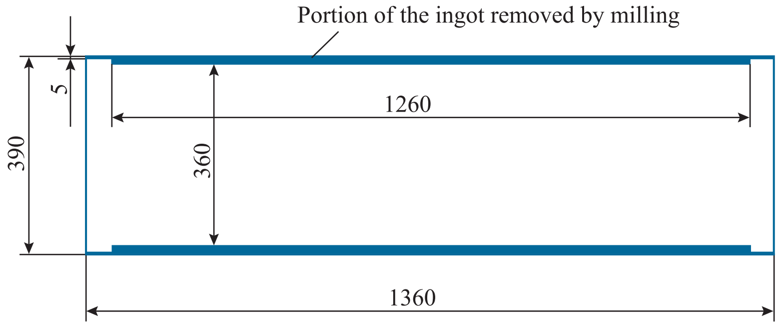

Fig. 13. Portion of the ingot surface to be removed by milling in the new cladding scheme

Рис. 13. Удаляемая фрезерованием часть слитка при реализации новой схемы плакирования

Conclusions

1. A finite-element analysis was carried out to assess the technological feasibility of implementing a new cladding scheme for aluminum—lithium alloy 1441 ingots. Instead of the traditional scheme, which involves roll-bonding of cladding plates to the ingot in four passes with absolute reductions of 6 mm per pass, the new approach proposes placing the plates into pre-machined recesses on the upper and lower surfaces of the ingot and achieving roll-bonding in a single pass with an absolute reduction of 24 mm.

2. The new cladding scheme makes it possible to significantly reduce the total number of passes and inter-pass pauses during rough rolling, thereby improving the thermal condition of the workpiece before finish rolling. It is expected that the higher temperature will reduce the likelihood of edge cracking during finish rolling. A reduction of three passes and three 10-second pauses increases the mean temperature by approximately 23 °C.

3. The proposed scheme prevents extrusion of the cladding plates from the ingot surface even at high absolute reductions. This allows the use of thinner cladding plates — 10 mm instead of the conventional 15 mm.

4. The deformation state of the base metal (alloy 1441) and the cladding layer (ACpl alloy) differs substantially between the two schemes. The mean accumulated strain in the ingot after four passes with 6 mm reductions was 0.05, while after a single-pass rolling with a 24 mm reduction it doubled to 0.10. At the same time, deformation of the cladding layer in the new scheme was more uniform.

5. The results of the finite-element modeling can be used to improve and optimize the technological parameters of hot rolling for clad sheets and strips made of aluminum—lithium alloy 1441 under the production conditions of KUMZ JSC.

References

1. Betsofen S.Ya., Antipov V.V., Knyazev M.I. Al—Cu—Li and Al—Mg—Li alloys: Phase composition, texture, and anisotropy of mechanical properties (Review). *Russian Metallurgy (Metally)*. 2016;2016:326—341. https://doi.org/10.1134/S0036029516040042
2. Rioja R.J., Liu J. The evolution of Al—Li base products for aerospace and space applications. *Metallurgical and Materials Transactions A*. 2012;43:3325—3337. https://doi.org/10.1007/s11661-012-1155-z
3. El-Aty A.A., Xu Y., Guo X., Zhang S.-H., Ma Y., Chen D. Strengthening mechanisms, deformation behavior, and anisotropic mechanical properties of Al—Li alloys: A review. *Journal of Advanced Research*. 2018;10:49—67. https://doi.org/10.1016/j.jare.2017.12.004
4. Antipov V.V., Tkachenko E.A., Zaitsev D.V., Selivanov A.A., Ovsyannikov B.V. Influence of homogenization annealing modes on the structural-phase state and mechanical properties of ingots made of aluminum-lithium alloy 1441. *Trudy VIAM*. 2019;3(75):44—52. (In Russ.). https://doi.org/10.18577/2307-6046-2019-0-3-44-52
   Антипов В.В., Ткаченко Е.А., Зайцев Д.В., Селиванов А.А., Овсянников Б.В. Влияние режимов гомогенизационного отжига на структурно-фазовое состояние и механические свойства слитков из алюминий-литиевого сплава 1441. *Труды ВИАМ*. 2019;3(75):44—52. https://doi.org/10.18577/2307-6046-2019-0-3-44-52
5. Li H., Zou Z., Li J., Xu G., Zheng Z. Correlation between grain structures and tensile properties of Al—Li alloys. *Transactions of Nonferrous Metals Society of China*. 2023;33(12):3597—3611. https://doi.org/10.1016/S1003-6326(23)66357-5
6. Ovsyannikov B.V. New aluminum-lithium alloy of the Al—Cu—Mg—Li(Ag,Sc) system intended for the

production of thin sheets and profiles. *Non-Ferrous Metals*. 2014;(11):90—94. (In Russ.).
Овсянников Б.В. Новый алюминиево-литиевый сплав системы А—Cu—Mg—Li(Ag,Sc), предназначенный для изготовления тонких листов и профилей. *Цветные металлы*. 2014;(11):90—94.

7. Kokovin P.L., Maltseva T.V., Ovsyannikov B.V. Mastering the technology of casting large-sized flat ingots from a new generation aluminum-lithium alloy. *Liteishchik Rossii*. 2023;(1):21—24. (In Russ.).
Коковин П.Л., Мальцева Т.В., Овсянников Б.В. Освоение технологии литья крупногабаритных плоских слитков из алюминиево-литиевого сплава нового поколения. *Литейщик России*. 2023;(1):21—24.
8. Ovsyannikov B.V., Komarov S.B. Development of production of deformed semi-finished products from aluminum-lithium alloys at JSC “KUMZ”. *Tekhnologiya legkikh splavov*. 2014;(1):97—103. (In Russ.).
Овсянников Б.В., Комаров С.Б. Развитие производства деформированных полуфабрикатов из алюминиево-литиевых сплавов в ОАО «КУМЗ». *Технология легких сплавов*. 2014;(1):97—103.
9. Hajjioui E.A., Bouchaala K., Faqir M., Essadiqi E. A review of manufacturing processes, mechanical properties and precipitations for aluminum lithium alloys used in aeronautic applications. *Heliyon*. 2023;9(3):e12565. https://doi.org/10.1016/j.heliyon.2022.e12565
10. Duan S.Y., Huang L.K., Yang S.H., Zhou Z., Song S.J., Yang X.B., Chen Y.Z., Li Y.J., Liu G., Liu F. Uncovering the origin of enhanced strengthening in Li-added Al—Cu—Mg alloys. *Materials Science and Engineering: A*. 2021;827:142079.
https://doi.org/10.1016/j.msea.2021.142079
11. Rioja R.J., Liu J. The evolution of Al—Li base products for aerospace and space applications. *Metallurgical and Materials Transactions A*. 2012;43(9):3325—3337.
https://doi.org/10.1007/s11661-012-1155-z
12. First-principles insights into solute partition among various nano-phases in Al—Cu—Li—Mg alloys. *Transactions of Nonferrous Metals Society of China*. 2024:34(6): 1734—1744.
https://doi.org/10.1016/S1003-6326(24)66503-9
13. Kolobnev N.I., Khokhlatova L.B., Antipov V.V. Promising aluminum-lithium alloys for aircraft structures. *Tekhnologiya legkikh splavov*. 2007;(2):35—38. (In Russ.).
Колобнев Н.И., Хохлатова Л.Б., Антипов В.В. Перспективные алюминий-литиевые сплавы для самолетных конструкций. *Технология легких сплавов*. 2007;(2):35—38.
14. Pantelakis S.G., Chamos A.N., Setsika D. Tolerable corrosion damage on aircraft aluminum structures: Local cladding patterns. *Theoretical and Applied Fracture Mechanics*. 2012;58(1):55—64.
https://doi.org/10.1016/j.tafmec.2012.02.008
15. Corrosion of aluminum and aluminum alloys. Ed. D.R. Davis. Transl. Yu.I. Kuznetsov, M.Z. Lokshin. Moscow: NP «APRAL», 2016. 333 p. (In Russ.).
Коррозия алюминия и алюминиевых сплавов. Под ред. Д.Р. Дэйвиса. Пер. с англ. Ю.И. Кузнецова, М.З. Локшина. М.: НП «АПРАЛ», 2016. 333 с.
16. Razinkin A.V., Maltseva T.V., Ovsyannikov B.V., Levina A.V. Typical defects in ingots and semi-finished products made of aluminum deformable alloys. Ekaterinburg: Uralskii rabochii, 2023. 144 p. (In Russ.).
Разинкин А.В., Мальцева Т.В., Овсянников Б.В., Левина А.В. Типовые дефекты в слитках и полуфабрикатах из алюминиевых деформируемых сплавов. Екатеринбург: Уральский рабочий, 2023. 144 с.
17. Degtyarev A.V., Maltseva T.V., Glinskikh P.I., Yakovlev S.I. Technological features of production of clad sheets from hard aluminum alloys at JSC “KUMZ”. *Tekhnologiya legkikh splavov*. 2024;(2):40—46 (In Russ.).
https://doi.org/10.24412/0321-4664-2024-2-40-46
Дегтярев А.В., Мальцева Т.В., Глинских П.И., Яковлев С.И. Технологические особенности производства плакированных листов из твердых алюминиевых сплавов в ОАО «КУМЗ». *Технология легких сплавов*. 2024;(2):40—46.
https://doi.org/10.24412/0321-4664-2024-2-40-46
18. Orlov V.K., Drozd V.G., Sarafanov M.A., Specific features of aluminum alloy plates rolling. *Proizvodstvo prokata*. 2016;(4):11—16. (In Russ.).
Орлов В.К., Дрозд В.Г., Сарафанов М.А. Особенности прокатки плит из алюминиевых сплавов. *Производство проката*. 2016;(4):11—16.
19. Yashin V.V., Beglov E.D., Aryshensky E.V., Latushkin I.A. Effect of cladding layer thickness on deformation distribution over ingot cross-section. In: *IX International congress "Non-ferrous metals and minerals-2017"* (Krasnoyarsk, 11–15 September 2017). Krasnoyarsk, 2017. P. 735–744. (In Russ.).
Яшин В.В., Беглов Э.Д., Арышенский Е.В., Латушкин И.А. Влияние толщины плакирующего слоя на распределение деформации по сечению слитка. В сб.: *IX Международный конгресс «Цветные металлы и минералы-2017»* (Красноярск, 11—15 сент. 2017). Красноярск, 2017. С. 735—744.
20. Torikai G., Yoshida Y., Asano M., Niikura A. Visualization of metal flow and adhering of aluminum alloy in three-layer clad rolling. *Procedia Manufacturing*. 2018;15: 144—151.
https://doi.org/10.1016/j.promfg.2018.07.188

21. Puchkova L.M. Features of joint rolling of high layered strips of different-strength metals. *Proizvodstvo prokata.* 2014;(9):3—10. (In Russ.).
Пучкова Л.М. Особенности совместной прокатки высоких слоистых полос разнопрочных металлов. *Производство проката.* 2014;(9):3—10.
22. Khan H.A., Asim K., Akram F., Hameed A., Khan A., Mansoor B. Roll bonding processes: State-of-the-art and future perspectives. *Metals.* 2021;11(9):1344.
https://doi.org/10.3390/met11091344
23. Zixuan L., Shahed R., Tao W., Han J., Shu X., Pater Z., Huang Q. Recent advances and trends in roll bonding process and bonding model: A review. *Chinese Journal of Aeronautics.* 2023;36(4):36—74.
https://doi.org/10.1016/j.cja.2022.07.004
24. Kebriaei R., Vladimirov I.N., Reese S. Joining of the alloys AA1050 and AA5754 — Experimental characterization and multiscale modeling based on a cohesive zone element technique. *Journal of Materials Processing Technology.* 2014;214(10):2146—2155.
https://doi.org/10.1016/j.jmatprotec.2014.03.014
25. Salikhyanov D.R. Investigation of the stress-strain state at the boundary between materials during rolling of a layered composite. *Ferrous Metals.* 2023;(9):34—39. (In Russ.). https://doi.org/10.17580/chm.2023.09.06
Салихянов Д.Р. Исследование напряженно-деформированного состояния на границе между материалами при прокатке слоистого композита. *Черные металлы.* 2023;(9):34—39.
26. Koshmin A., Zinoviev A., Cherkasov S., Ali Alhaj A.M., Tsydenov K., Churyumov A. Finite element modeling and experimental verification of a new aluminum Al—2%Cu—2%Mn alloy hot cladding by flat rolling. *Metals.* 2024;14(8):852.
https://doi.org/10.3390/met14080852
27. Zinyagin A.G., Borisenko N.R., Muntin A.V., Kryuchkova M.O. Features of finite element modeling for hot rolling process of clad sheets and strips. *CIS Iron and Steel Review.* 2023;26(2):51—57.
https://doi.org/10.17580/cisisr.2023.02.08
28. Vlasov A.V., Stebunov S.A., Evsyukov S.A., Biba N.V., Shitikov A.A. Finite element modeling of technological processes of forging and bulk stamping: a tutorial. Moscow: Publ. House of the Bauman MSTU, 2019. 384 p. (In Russ.).
Власов А.В., Стебунов С.А., Евсюков С.А., Биба Н.В., Шитиков А.А. Конечно-элементное моделирование технологических процессов ковки и объемной штамповки: Учеб. пос. М.: Изд-во МГТУ им. Н.Э. Баумана, 2019. 384 с.

Information about the authors

Aleksandr M. Pesin – Dr. Sci. (Eng.), Prof., Chief Researcher of the Laboratory of Mechanics of Gradient Nanomaterials n.a. A.P. Zhilyaev, Nosov Magnitogorsk State Technical University (NMSTU).
https://orcid.org/0000-0002-5443-423X
E-mail: pesin@bk.ru

Aleksandr V. Razinkin – Cand. Sci. (Eng.), Director of Production, PJSC “Kamensk-Uralsky Metallurgical Plant” (PJSC “KUMP”).
https://orcid.org/0009-0006-2851-227X
E-mail: RazinkinAV@kumz.ru

Vladimir A. Zamaraev – Engineer, PJSC “KUMP”.
https://orcid.org/0009-0006-6743-9212
E-mail: zamaraevva@kumw.ru

Denis O. Pustovoitov – Cand. Sci. (Eng.), Associate Professor, Leading Researcher of the Laboratory of Mechanics of Gradient Nanomaterials n.a. A.P. Zhilyaev, NMSTU.
https://orcid.org/0000-0003-0496-0976
E-mail: pustovoitov_den@mail.ru

Информация об авторах

Александр Моисеевич Песин – д.т.н., профессор, гл. науч. сотрудник лаборатории «Механика градиентных материалов им. А.П. Жиляева» Магнитогорского государственного технического университета (МГТУ) им. Г.И. Носова.
https://orcid.org/0000-0002-5443-423X
E-mail: pesin@bk.ru

Александр Викторович Разинкин – к.т.н., директор по производству ПАО «Каменск-Уральский металлургический завод» (ПАО «КУМЗ»).
https://orcid.org/0009-0006-2851-227X
E-mail: RazinkinAV@kumz.ru

Владимир Андреевич Замараев – инженер-технолог ПАО «КУМЗ».
https://orcid.org/0009-0006-6743-9212
E-mail: zamaraevva@kumw.ru

Денис Олегович Пустовойтов – к.т.н., доцент, вед. науч. сотрудник лаборатории «Механика градиентных материалов им. А.П. Жиляева» МГТУ им. Г.И. Носова.
https://orcid.org/0000-0003-0496-0976
E-mail: pustovoitov_den@mail.ru

Contribution of the authors

A.M. Pesin – proposed the new cladding scheme for aluminum–lithium alloy 1441 ingots, participated in the discussion of the results.

A.V. Razinkin – defined the aim of the study, specified the initial and boundary conditions for modeling the ingot cladding process, participated in the discussion of the results.

V.A. Zamaraev – prepared specimens and obtained experimental flow-stress data for alloy 1441, participated in the discussion of the results.

D.O. Pustovoitov – performed finite-element modeling of the ingot cladding process in QForm, participated in the discussion of the results, wrote the manuscript.

Вклад авторов

А.М. Песин – предложение новой схемы плакирования слитков из алюминий-литиевого сплава 1441, участие в обсуждении результатов.

А.В. Разинкин – определение цели работы, задание начальных и граничных условий для моделирования процесса плакирования слитков, участие в обсуждении результатов.

В.А. Замараев – приготовление образцов и получение экспериментальных данных о сопротивлении деформации сплава 1441, участие в обсуждении результатов.

Д.О. Пустовойтов – моделирование процесса плакирования слитков методом конечных элементов в программе «QForm», участие в обсуждении результатов, написание статьи.

The article was submitted 13.09.2024, revised 11.03.2025, accepted for publication 13.03.2025

Статья поступила в редакцию 13.09.2024, доработана 11.03.2025, подписана в печать 13.03.2025